

# Novel Symmetry-preserving Neural Network Model for Phylogenetic Inference

Xudong Tang<sup>\*</sup>

Wisconsin Institute for Discovery  
University of Wisconsin-Madison  
Madison, WI 53706

Leonardo Zepeda-Nuñez<sup>\*,†</sup>

Department of Mathematics  
University of Wisconsin-Madison  
Madison, WI 53706

Shengwen Yang

Department of Statistics  
University of Wisconsin-Madison  
Madison, WI 53706

Zelin Zhao

Department of Mathematics  
University of Wisconsin-Madison  
Madison, WI 53706

Claudia Solís-Lemus<sup>‡</sup>

Wisconsin Institute for Discovery  
University of Wisconsin-Madison  
Madison, WI 53706

## ABSTRACT

Scientists world-wide are putting together massive efforts to understand how the biodiversity that we see on Earth evolved from single-cell organisms at the origin of life and this diversification process is represented through the Tree of Life. Low sampling rates and high heterogeneity in the rate of evolution across sites and lineages produce a phenomenon denoted “long branch attraction” (LBA) in which long non-sister lineages are estimated to be sisters regardless of their true evolutionary relationship. LBA has been a pervasive problem in phylogenetic inference affecting different types of methodologies from distance-based to likelihood-based. Here, we present a novel neural network model that outperforms standard phylogenetic methods and other neural network implementations under LBA settings. Furthermore, unlike existing neural network models, our model naturally accounts for the tree isomorphisms via permutation invariant functions which ultimately result in lower memory and allows the seamless extension to larger trees.

**Keywords** phylogenetic tree · protein sequence evolution · long-branch attraction · recurrent network · tree isomorphisms

## 1 Introduction

The Tree of Life is the representation of the evolutionary process that originated the world-wide diversity of life from single-cell organisms. Existing approaches to reconstruct the Tree of Life

<sup>\*</sup>Equal contribution; authors in alphabetical order

<sup>†</sup>Now at Google Research

<sup>‡</sup>Corresponding author: solislemus@wisc.edu

involve the collection of genomic data from living organisms, and then, the fit of statistical techniques to estimate the tree structure which is in agreement with the observed genomic data under a specified model of evolution. While the cost of sequencing collected organisms continues to decrease, many clades in the tree still do not have a high sampling proportion due to limited or inaccessible species ranges or poor allocation of resources. Furthermore, out of the 1.4 million estimated species, it is estimated that there are from 10 to 100 million undiscovered and undescribed species [1].

Low sampling of species can cause long branches in the tree which could be incorrectly grouped in a phenomenon denoted “long branch attraction” (LBA) [2, 3, 4, 5] where long branches in the tree are estimated to be sisters regardless of their true evolutionary relationship. More formally, LBA arises when the probability that close relatives share character states due to common ancestry is exceeded by the probability that more distantly related taxa share states due to convergent evolution [2]. It has been studied that increasing the sampling frequency can potentially divide those long branches and thus, overcome the LBA problem [6, 7], yet it is not always possible to increase sampling of some clades in the Tree of Life.

Aside from low sampling, LBA also arises when there are inequalities in the rate of evolution among branches [3]. In this scenario, commonly referred to as “Felsenstein zone” [8, 9], an incorrect tree that groups taxa belonging to high-rate lineages will be more likely to be estimated as more data are accumulated. This implies that LBA would appear in rapidly evolving lineages (like virus or bacteria) which produce long branches leading to some taxa which are then artificially estimated as sister taxa by most traditional phylogenetic methods. These traditional methods tend to ignore heterogeneities such as within-site rate variation (heterotachy) [10] or rate variation across lineages. Site-heterogeneous models [11] that allow different rates of mutation for different sites have successfully overcome LBA for some datasets [12]. Yet the complexity to infer site-heterogeneous models has hampered its use for large datasets with many sites and many taxa.

The first implementations of neural network models in phylogenetic inference [13, 14, 15] have found that neural networks are able to accurately estimate phylogenetic trees with long branches and thus, overcome the LBA phenomenon. These implementations share three similarities: 1) they all focus on neural network models (mainly CNNs); 2) they can only estimate 4-taxon trees, and 3) they have been proven to outperform standard phylogenetic inference methods like maximum likelihood, bayesian inference and maximum parsimony under a variety of heterogeneous simulated scenarios, especially those related to the anomaly zone (LBA) [14, 15], Felsenstein trees, Farris trees [13] or scenarios with highly gapped alignments [14].

The main shared weakness of these phylogenetic neural network models is their limitation to 4-taxon datasets. While Zou *et al* [15] was able to analyze larger real datasets in combination with Quartet Puzzling [16], extending the neural network model to  $n$  taxa would allow a direct estimation of a  $n$ -taxon tree as opposed to breaking up an  $n$ -taxon dataset into all combinations of 4 taxa to later merge the resulting quartets. One of the challenges to extend these neural network models to more taxa is the symmetric nature of the tree structure. For example, in the quartet  $((A, B), (C, D))$ , the sequences A and B (and the sequences C and D) are interchangeable, as are the clades  $(A, B)$  and  $(C, D)$  with  $((C, D), (A, B))$  or  $((C, D), (B, A))$  representing the same tree structure. Zou *et al* [15] account for all the symmetries by artificially creating all 24 permutations of the sequences to guarantee that their neural network model is invariant to the symmetries. This process, however, is not scalable for larger trees both in terms of computing time and memory allocation for all the artificial permutations. More recent implementations of neural networks in phylogenetics can estimate trees with up to 15 taxa [17], yet this model relies on comparing simulated data with real data, rather than classifying the best tree.

Here, we exploit the inherent symmetries of the tree objects with the first symmetry-preserving neural network model which provides a classification framework that can be extended to more than four taxa. We show that our NN model not only outperforms standard phylogenetic inference methods like neighbor joining, maximum likelihood and Bayesian inference, it also outperforms existing neural network models [15] all while reducing the memory needs and training time by not requiring the creation of artificial permutations of the data. Our work opens the door to neural

network models capable of directly classifying  $n$ -taxon trees through the invariant transformations that are built into our model.

## 2 Description of symmetry-preserving neural network model for four taxa

The particular structure of our proposed method leverages two main features of the problem: the positional information within the sequence and the equivariance of the tree-topology with respect to the order of the sequences. These two main features are then embedded within the architecture of the network. In what follows we will describe in general terms the architecture and how is able to preserve the two properties mentioned above. For the sake of clarity, we will present them in a modular fashion, similarly as it is implemented in the code.

**Symmetry-preserving neural network.** Even though the number of possible trees increases exponentially with the number of species, there exist several symmetries that one can leverage. Suppose that we have four different species, denoted A, B, C, and D, and for each of these species we have data in the form of sequences  $s_A, s_B, s_C$ , and  $s_D$ . The task at hand is to estimate the most likely tree topology that explains the data fed as a matrix of the form  $[s_A, s_B, s_C, s_D]$ . In this case of four taxa, we only have *three* possible unrooted tree topologies which are depicted in Fig. 1 (top). We then seek a function  $p([s_A, s_B, s_C, s_D]) \rightarrow [p_I, p_{II}, p_{III}]$ , where  $p_I$  is the probability that the data is explained by the tree of type I (and similarly for  $p_{II}$  and  $p_{III}$ ). Even though we can obtain 24 different trees with four leaves by permutation of the leaf labels, many of these are equivalent in the sense that they share the same labelled topology, as shown in Fig. 1 (bottom).

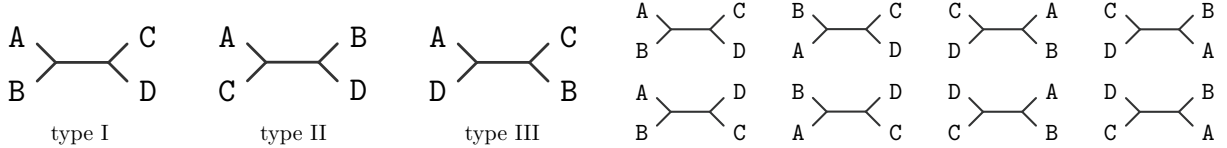


Figure 1: Top: Possible unrooted trees for 4 species (quartets). Bottom: All the possible permutations on the order of the leaves that are isomorphic to a tree of type I.

This simple example already sheds light on the properties we will exploit to reduce the search space. The order in which the input is fed is completely arbitrary, and it is subject to several invariances. For example, if the tree to be estimated is of type I, then exchanging the position of A and B (or C and D) leads to the same topology (Fig. 1 top). Thus, if we were to feed our algorithm the data ordered as  $[s_B, s_A, s_C, s_D]$ , or alternatively as  $[s_A, s_B, s_D, s_C]$ , we would expect the score  $p_I$  to be the same. In addition, if we exchange each clade, i.e., we swap A and B by C and D, then the topology remains the same, and so should the score  $p_I$ . In addition, if one tree is predicted to be certain type, and then we permute the order in which the sequences are feed, it may change the type that was predicted originally. In fact, there is a correspondence between how the labels should be modified under any permutation of the sequences.

Creating a network that is invariant to these transformations will reduce the number of parameters, the number of data points necessary for training, and hence the computational cost. More formally, we will take advantage of the newly developed theory of invariant networks [18], which states that any permutation invariant function  $f : \mathbb{R}^n \rightarrow \mathbb{R}$  accepts a representation of the form

$$f(x_1, x_2, x_3, \dots, x_n) = \Phi \left( \sum_{i=1}^n \phi(x_i) \right)$$

where

$$\begin{aligned} \phi : \mathbb{R} &\rightarrow \mathbb{R}^m \\ \Phi : \mathbb{R}^m &\rightarrow \mathbb{R} \end{aligned}$$

where  $m$  is the embedding dimension, which is case dependent. In this case, we will exploit this property and extend it to the case of phylogenetic trees.

For example, suppose that  $\phi : \mathbb{D}^L \rightarrow \mathbb{R}^{L \times m}$ , where  $\mathbb{D}$  is the dictionary for the sequences (e.g., the set of nucleotides or aminoacids), and  $L$  is the sequence length. Suppose that  $\Phi : \mathbb{R}^{L \times m} \rightarrow \mathbb{R}^{L \times m}$ , then we have that  $\Phi(\phi(s_A) + \phi(s_B))$  will be invariant if we permute A and B, and  $\Phi(\phi(s_C) + \phi(s_D))$  will be invariant if we permute C and D.

Then, we define the descriptor

$$\begin{aligned} \mathcal{D}_I([s_A, s_B, s_C, s_D]) &= \Phi(\phi(s_A) + \phi(s_B)) \\ &\quad + \Phi(\phi(s_C) + \phi(s_D)) \end{aligned}$$

which is clearly invariant to the transformations which are invariant for the tree of type I.

Thus, if we have a third function  $\Psi : \mathbb{R}^{L \times m} \rightarrow [0, 1]$ , and we can write

$$\begin{aligned} p_I([s_B, s_A, s_C, s_D]) &= \Psi(\Phi(\phi(s_A) + \phi(s_B)) + \Phi(\phi(s_C) + \phi(s_D))) \\ &= \Psi(\mathcal{D}_I([s_B, s_A, s_C, s_D])) \end{aligned}$$

which is a score function that satisfies all the symmetries required. We use the same strategy to define the scores for trees of type II and III, resulting in

$$\begin{aligned} p_{II}([s_B, s_A, s_C, s_D]) &= \Psi(\Phi(\phi(s_A) + \phi(s_C)) \\ &\quad + \Phi(\phi(s_B) + \phi(s_D))), \\ p_{III}([s_B, s_A, s_C, s_D]) &= \Psi(\Phi(\phi(s_A) + \phi(s_D)) \\ &\quad + \Phi(\phi(s_C) + \phi(s_B))). \end{aligned}$$

The scores can be written in a more compact fashion by aggregating them into a vector:

$$p([s_B, s_A, s_C, s_D]) = \begin{bmatrix} p_I \\ p_{II} \\ p_{III} \end{bmatrix} = \begin{bmatrix} \Psi(\mathcal{D}_I([s_A, s_B, s_C, s_D])) \\ \Psi(\mathcal{D}_{II}([s_A, s_B, s_C, s_D])) \\ \Psi(\mathcal{D}_{III}([s_A, s_B, s_C, s_D])) \end{bmatrix} \quad (1)$$

where the descriptors are given by

$$\begin{bmatrix} \mathcal{D}_I \\ \mathcal{D}_{II} \\ \mathcal{D}_{III} \end{bmatrix} = \begin{bmatrix} \Phi(\phi(s_A) + \phi(s_B)) + \Phi(\phi(s_C) + \phi(s_D)) \\ \Phi(\phi(s_A) + \phi(s_C)) + \Phi(\phi(s_B) + \phi(s_D)) \\ \Phi(\phi(s_A) + \phi(s_D)) + \Phi(\phi(s_C) + \phi(s_B)) \end{bmatrix}. \quad (2)$$

This scoring function satisfies all the symmetries, and it only requires us to find three functions, which will be parametrized using NNs. This technique can be generalized to larger numbers of species seamlessly.

In what follows we provide extra details on how the descriptor  $\mathcal{D}$  and the scoring function  $\Psi$  are implemented.

**Symmetry-preserving descriptors.** We now provide the exact form of the descriptors for each tree topology. The main motivation of each descriptor is to respect both the symmetries and the ordering imposed by the sequences. In a nutshell, the descriptor will apply the same transformation to each site but across the four sequences independently of the rest of the sites. In a nutshell, the  $i$ -th slice of the descriptor will only depend on the  $i$ -th site of the input sequences.

In particular, the descriptor take an input of the form

$$\mathcal{D}_I : \mathbb{D}^{L \times 4} \rightarrow \mathbb{R}^{L \times m}$$

by applying the same transformation to each of the slices of the input  $[s_A, s_B, s_C, s_D]$  independently.

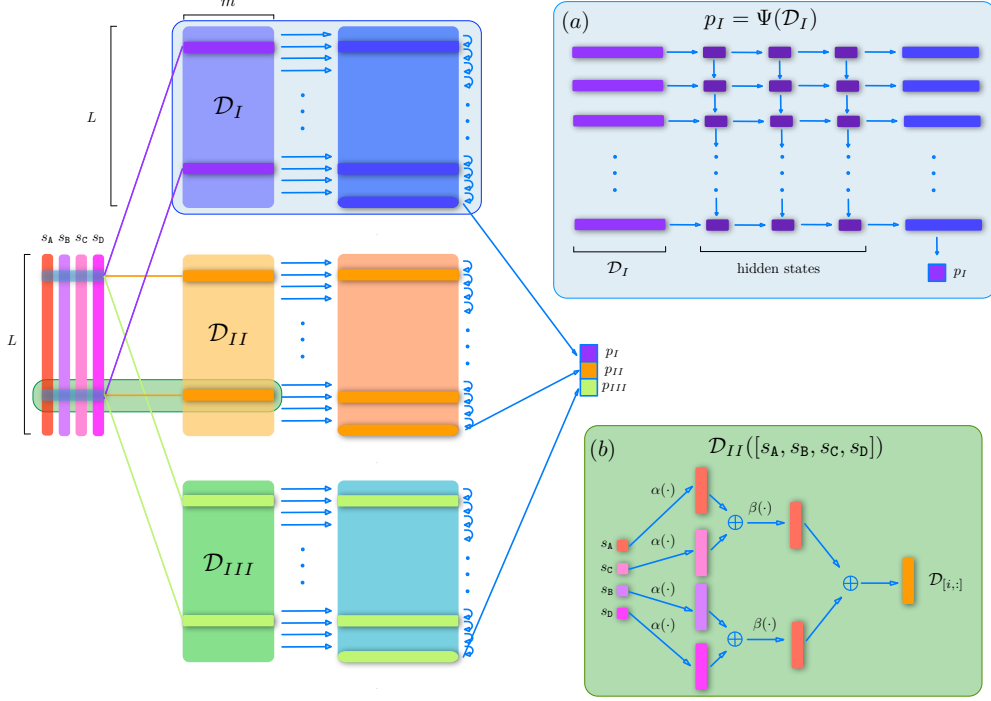


Figure 2: Diagram of the network. We start with sequences  $[s_A, s_B, s_C, s_D]$  in the left, then we apply the same functions  $\phi$  and  $\Phi$ , but in a different order to obtain the descriptors  $\mathcal{D}_I$ ,  $\mathcal{D}_{II}$ , and  $\mathcal{D}_{III}$ , which are described in (b). Then each descriptor is fed to the function  $\Psi$  (shown in (a)) which outputs the score for each particular tree topology. (a) Diagram of  $\Psi$  which is described by a LSTM followed by a dense network. (b) Diagram of the computation of a slice of  $\mathcal{D}_{II}$ , relying on the functions  $\alpha$ , which is an embedding layer, and  $\beta$ , which is a shallow dense ResNet.

By the sake of simplicity, we will denote by a generic  $s \in \mathbb{D}^L$  one of the four sequences mentioned before and  $s_i \in \mathbb{D}$  its  $i$ -th component (or site).

As shown in Fig. 2 (b), the first operation is an embedding layer, which will use the map  $\alpha : \mathbb{D} \rightarrow \mathbb{R}^m$ , and it will be applied to each site of the sequence, i.e., the function  $\phi$  mentioned above:=

$$(\phi(s))_{[i,:]} = \alpha(s_i)$$

where we have used Matlab notation (i.e., if  $A \in \mathbb{R}^{m \times m}$  then  $A_{[i,:]}$  corresponds to the  $i$ -th row of  $A$ ).

Then, we can do the same for  $\Phi$ , which will be written as the application of a function  $\beta : \mathbb{R}^m \rightarrow \mathbb{R}^m$  to each slice of the output of  $\phi$ , i.e.,

$$\begin{aligned} (\Phi(\phi(s) + \phi(s')))_{[i,:]} &= \beta \left( (\phi(s)_{[i,:]} + \phi(s')_{[i,:]}) \right) \\ &= \beta(\phi(s)_{[i,:]} + \phi(s')_{[i,:]}) \\ &= \beta(\alpha(s_i) + \alpha(s'_i)). \end{aligned}$$

Then, we can write a generic descriptor by slice as

$$\mathcal{D}_{[i,:]} = \beta(\alpha(s_i) + \alpha(s'_i)) + \beta(\alpha(\tilde{s}_i) + \alpha(\hat{s}_i)),$$

where  $s, s', \tilde{s}$ , and  $\hat{s}$  are a certain ordering of the generic sequences  $s_A, s_B, s_C$ , and  $s_D$ , operation depicted in Fig. 2 (b).

We add the correct ordering of the sequences to take place in the expression above. This produces three different sequences of descriptors, each one of dimension  $L \times m$ . In this case,  $\alpha$  is implemented

by a embedding layer. This choice allows us to avoid the hot-encoding, which allows in turn to feed the data to the network more efficiently. On the other hand,  $\beta$  is implemented by dense ResNet block [19]. One could add a deeper network for the  $\alpha$  and  $\beta$  functions. However, empirically, we have found that gains seem to be marginal.

For simplicity  $\phi$  and  $\Phi$  are implemented with one-dimensional convolutions with a kernel size of one, instead a dense network. This produces the same effect as mentioned above, but allows us to avoid any unnecessary reshape and efficiently batch the computations.

We point out that the descriptors maintain the *order* in the sequence, which will be then leveraged by the recurrent network in what follows.

**Recurrent network.** Given the ordered nature of the data and the descriptor network that was built to preserve such order, the scoring function  $\Psi$  is implemented using a standard recurrent LSTM network [20] using the Pytorch built-in models to process the sequence of each descriptor to another sequence and then use the last element of the new sequence to compute the score as depicted in Fig. 2 (a).

As shown in Fig. 2 (a), the LSTM network takes each of the slices of the descriptor at each site, and the hidden states of the precedent slice, and outputs a new descriptor that contains the information of the current slice and the information carried over by the hidden states of the precedent slices, while preserving some of the information in a hidden state for the next slice. This is repeated throughout the sequence, resulting in a new sequence of descriptors in which at each site, unlike the input, has information about all the sites *before it* and thus accounting for correlation among sites in one direction. Then we only consider the last row (or slice) of the output of the LSTM, which is fed to a feed-forward neural network, and ultimately outputs one single number: the score of the network to be of certain tree type.

The same process is repeated for the descriptors of each type of tree in Equation 2 and their outputs are then concatenated, thus obtaining the scores following Equation 1, which is shown in Fig. 2.

**Loss function and optimizer.** We used a typical multi class cross entropy loss, and the optimizer used was Adam [21] with the default parameters in pytorch [22]. We used an exponential scheduler for the learning rate.

## 2.1 Extension to five taxa

Let A, B, C, D, and E be the five taxa with sequences  $s_A$ ,  $s_B$ ,  $s_C$ ,  $s_D$ , and  $s_E$ . While for four taxa there are 3 possible unrooted tree topologies, there are now 15 possibilities for the case of five taxa (Fig. 3). We can group these trees by the one species in the middle (in Fig. 3, it is taxon E) having three different topologies.

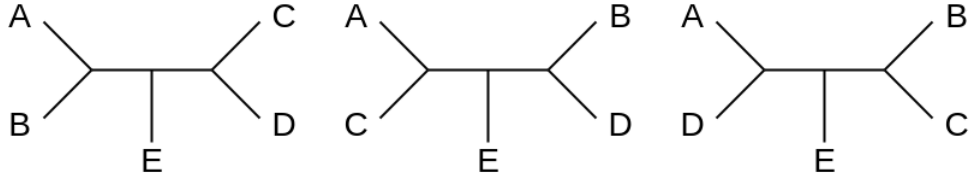


Figure 3: Three possible 5-taxon unrooted tree topologies out of the 15 possibilities. Note that we can still exploit the symmetry characteristic of these topologies.

We can still exploit the symmetric characteristic in quartet trees when working with quintet trees. For example, in Fig. 3, species E is in the middle. We could simply ignore species E and represent the two binary tree tips on both sides using  $\Phi$  and  $\phi$  functions as we did in the quartet tree cases. Essentially, we would create 15 descriptors on 15 quartet trees coming from the original 15 quintet

trees excluding the middle species as in Equation 3:

$$\begin{bmatrix} \mathcal{D}_I \\ \mathcal{D}_{II} \\ \mathcal{D}_{III} \\ \mathcal{D}_{IV} \\ \dots \\ \mathcal{D}_{XV} \end{bmatrix} = \begin{bmatrix} \Phi(\phi(s_A) + \phi(s_B)) + \Phi(\phi(s_C) + \phi(s_D)) \\ \Phi(\phi(s_A) + \phi(s_C)) + \Phi(\phi(s_B) + \phi(s_D)) \\ \Phi(\phi(s_A) + \phi(s_D)) + \Phi(\phi(s_C) + \phi(s_B)) \\ \Phi(\phi(s_A) + \phi(s_B)) + \Phi(\phi(s_C) + \phi(s_E)) \\ \dots \\ \Phi(\phi(s_B) + \phi(s_C)) + \Phi(\phi(s_D) + \phi(s_E)) \end{bmatrix}. \quad (3)$$

The model components and structures are exactly the same as in Fig. 2 except now we have 15 Descriptors and 15  $p$  values.

## 2.2 Open-source implementation

Our NN model was implemented using Python leveraging Pytorch. We implement two version of the network, dubbed in what follows, LSTM and OptLSTM. The first one showcases the proposed network, whereas the second is an optimized version of the pipeline. All the scripts for the model implementation can be found in the GitHub repository: <https://github.com/crs14/nn-phylogenetics>.

## 3 Simulations

### 3.1 Simulation strategy on four taxa

We simulate protein sequences on known four-taxon trees. Then, we use the sequences as input data and the tree topology as labels to train the neural network model described in Section 2.

We follow the simulation procedure in [15]. Zou *et al* simulate protein sequences under the CTMC model and quartet gene trees, and then train a neural network model to classify sequences based on the quartet gene tree they came from. A tree out of the three possible unrooted quartets was selected at random and we simulate branch lengths under long-branch attraction cases: trees with two long branches, each sister to a short branch and separated by a short internal branch [23]). In this setting, we simulate the short external branches  $b = 0.1, 0.5, 1.0$  and then set the two long branches as  $a = \kappa_1 b$  for  $\kappa_1 = 2, 10, 40$  and the internal branch as  $c = \kappa_2 b$  for  $\kappa_2 = 0.01, 0.1, 1.0$  (see Fig. 4 top). These settings mimic the long-branch attraction simulations in [15].

The quartet was rooted in the internal branch always. A sequence of length  $L = 1550$  (randomly chosen length in the window  $(100, 3000)$  used in [15]) is simulated following a continuous-time Markov model using PAML [24, 25]. We use the amino acid substitution empirical model of Dayhoff [26] which was randomly chosen among the empirical models available in PAML. For every site, a relative evolutionary rate  $r$  was factored into the branch lengths. This rate was sampled from a uniform distribution in  $(0.05, 1.0)$  as in [15] and used in all the sites (that is, no site-specific rates were used).

The raw input data consisted in four amino acid sequences of length  $L$  which are fed through an embedding layer. Unlike [15], we do not have to permute the data to account for the symmetries. Our neural network model incorporates the symmetries directly (as described in the model description).

For these experiments we fixed the embedding dimension  $m = 80$ , and an hidden dimension of the LSTM network of 20, in which we used only three layers, including dropout layers with a drop out probability of 0.2, and RELU activation functions. We considered a batch size of 16.

In [15], the training data consisted of 100,000 samples, yet we used only 10,000 samples for our simulations and achieved comparable prediction accuracy (see Results). We compare the prediction accuracy of our neural network models described in Section 2 (LSTM and OptLSTM) with four phylogenetic inference methods: three standard phylogenetic methods 1) Neighbor-joining (NJ) [27, 28, 29]; 2) Maximum likelihood (ML) with RAxML [30]; 3) Bayesian inference (BI) with

MrBayes [31, 32], and 4) a previous neural network model by Zou *et al* [15]. Since the development of this work, two new neural network models have been published [14, 13], yet these two models were implemented for DNA sequences, not proteins, so we were unable to compare the performance of our models with these two neural network implementations (see Discussion).

In each experiment, we set the first 9,500 samples as the training data and the last 500 samples as the test data. For our implementation, we train the data for 100 epochs and test every 10 epochs to record the best accuracy and parameters of our model. We use the Adam optimizer with a learning rate of 0.001 to update our model and we decay the learning rate of each parameter group by 0.9 every 10 epochs. For the Zou NN implementation [15], we use the same parameters, except for the loss function: the reduction applied to the output is summed instead of averaged. For the three standard phylogenetic methods (NJ, ML, BI), we test on the last 500 samples.

We highlight that for the standard phylogenetic methods, we use the correct model specification. That is, we use the Dayhoff model to estimate the evolutionary distances in NJ, and we specify the substitution model to be Dayhoff for RAxML and MrBayes. This means that the performance of these methods reflects ideal conditions that are likely unattainable with real data for which the real model is unknown.

### 3.2 Results on four taxa

Fig. 4 (bottom) shows the performance of the six methods to estimate a 4-taxon quartet (top) under a variety of normal and LBA scenarios. We observe that for cases with low LBA ( $a = 2b, c = 1.0$ ), all six methods perform relatively well with testing accuracy of 100% in most cases. However, when the branch length  $a$  grows ( $a = 10b, 40b$ ), the standard phylogenetic methods (NJ, ML, BI) are no longer able to estimate the correct quartet tree with prediction accuracy of 0.0 in many of these cases. The neural network implementations, on the other hand, are able to recover the quartet tree even in extreme cases such as  $a = 40b, c = 0.1$ .

Among the neural network implementations, our model slightly outperforms Zou's [15], but while the improvement on prediction accuracy is small, our NN implementation is far more efficient in terms of memory given that we do not create all possible permutations of the input sequences. For example, our NN model used on average 8,487.3 mega bytes on estimation which is less than 8% of the memory used by the Zou's NN model (107,731.8 mega bytes on average). The efficiency also translated into faster estimation with an average of 4.36 hours to fit our NN implementation compared to 6.18 hours for the case of Zou's.

Fig. 5 shows the learning dynamics of our OptLSTM model on three chosen datasets:  $c = 1, b = 1$  with  $a = 2b, 10b, 40b$  that represent the three levels of LBA. In these plots, we present as dashed lines the final testing accuracies of the standard phylogenetic methods (NJ, ML, BI) and Zou's NN model. We also present as a gray dotted line the expected accuracy for a naive model that selects quartets at random (33% for 3 possible quartets).

For the case of low LBA ( $a = 2b$ ), our model reaches a testing accuracy of 100% rapidly and all methods in this case have a testing accuracy of 100% as well. As LBA worsens (left to right in Fig. 5), the testing accuracy decreases for all methods, but more dramatically for the standard phylogenetic methods (NJ, ML, BI) that have a testing accuracy of 0.0% (overlapped dashed lines at zero). Only the two NN models (Zou's and our OptLSTM) are able to reach a testing accuracy greater than the naive predictor with our model outperforming Zou's in both cases ( $a = 10b, 40b$ ).

### 3.3 Simulation strategy on five taxa

Since LBA is not a concern on more than four taxa, we use the same simulation strategy as with four taxa, but with a different setup for the branch lengths. We simulate branch lengths by uniformly sampling from  $(0, 1)$ . All other simulation parameters remain the same.

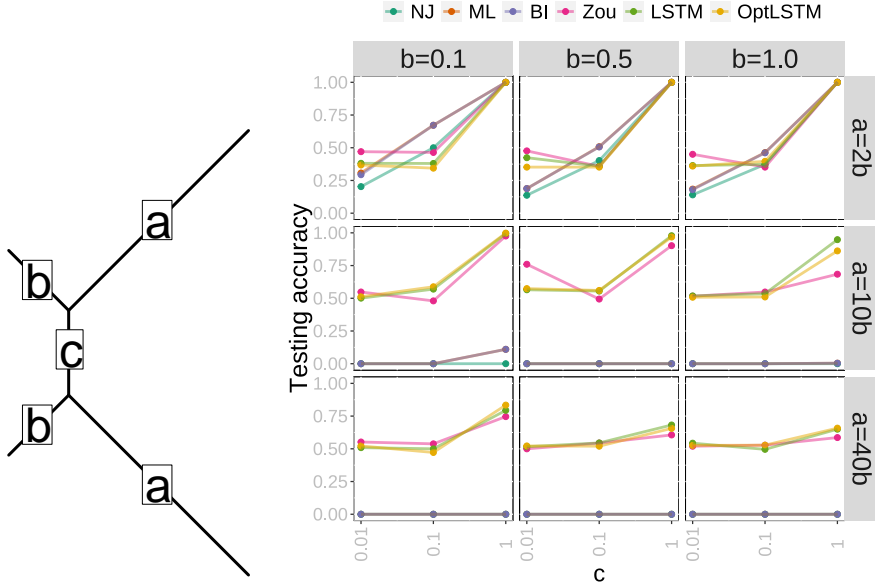


Figure 4: Comparison of testing accuracy for six methods: Neighbor-joining (NJ), Maximum Likelihood (ML), Bayesian Inference (BI), Neural Network model in [15] (Zou), our Neural Network models (LSTM and OptLSTM). We observe that neural network models (Zou, LSTM, OptLSTM) outperform standard phylogenetic inference methods (NJ, ML, BI) on LBA cases ( $a = 10b$ ,  $a = 40b$ ). Among those cases, our NN outperforms Zou’s with a slightly higher testing accuracy.

The hyperparameters of the model, however, are modified to achieve better performance. We increase the embedding dimension  $m$  from 80 to 160 and the hidden dimension of the LSTM network from 20 to 40, with 6 layers of LSTM instead of 3. We decrease the batch size from 16 to 8. These changes would increase the training time but could offer better model quality overall [33].

We use 10,000 samples for simulations to match the training set of quartet trees. Since the model in [15] could only work in a quartet tree setting, we could not conduct a comparison of performance like we did in the quartet tree case. While novel deep learning implementations are suitable for more than four taxa [17], the measurement metric is normalized Robinson-Foulds (RF) distance and loss, which are not comparable with our accuracy metric.

In this experiment, we take 1,000 samples from the training set to train the model for each epoch. While in theory having more training samples would result in better model quality, in practice, we find no significant difference in model performance between training with the whole set and training with a subset. Training with a subset vastly improves the training time. We test the model performance with 50 samples randomly selected every 10 epochs. The setting for the optimizer and learning rate is the same as the quartet tree cases. We train the model for a total of 1300 epochs.

### 3.4 Results on five taxa

Fig. 6 shows a maximum achieved accuracy of 0.72 with the best model, as shown by the red dashed line. We also show the result from standard phylogenetic methods (ML and NJ) with the black and green dashed lines. It is clear that in this case, the performance of our model is inferior to the standard phylogenetic methods, mostly due to the weakness of the classification task. While the performance is not as good as non-LBA cases for quartet trees, it is worth noting that the classification for a quintet tree is a much harder task than a quartet tree. For a quartet tree, the tree space is 3, thus the naive prediction of the model is 33%. For a quintet tree, the tree space increases

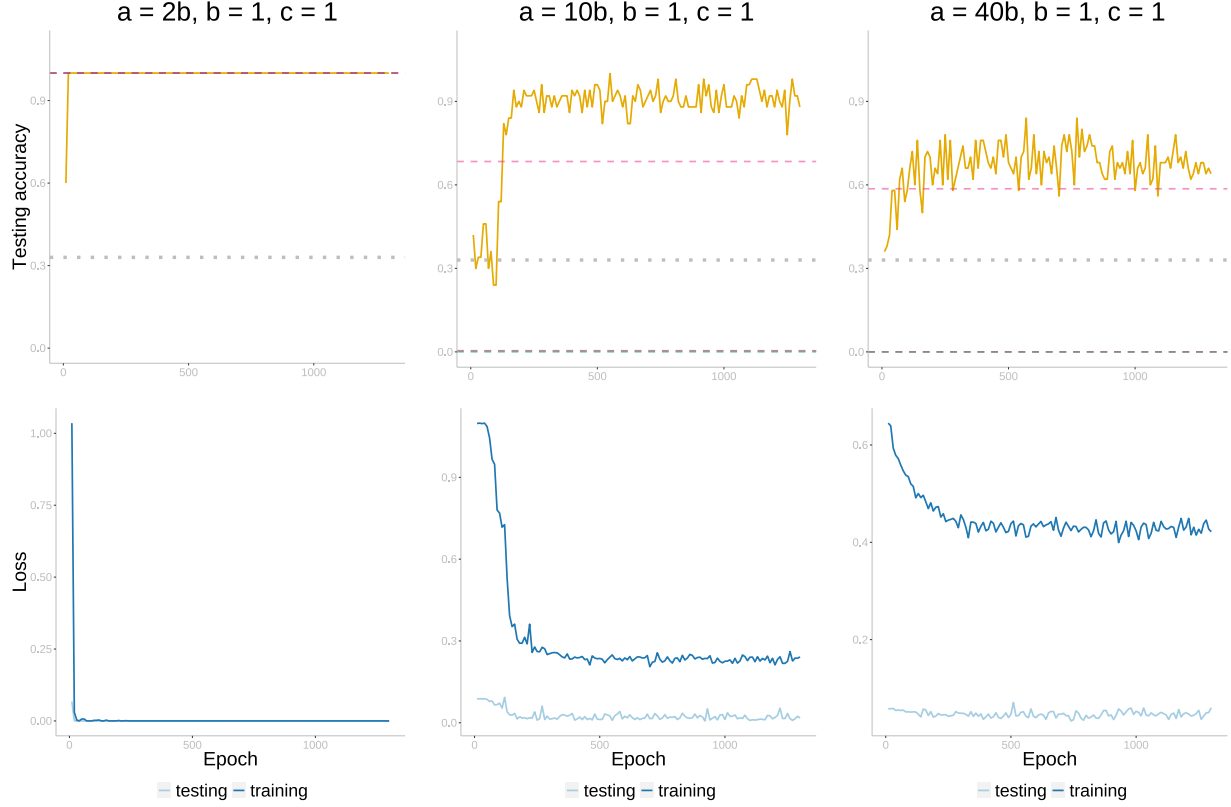


Figure 5: Testing accuracy and training/testing loss of our NN model implementation (OptLSTM) by epoch for three datasets of increased severity of LBA (left to right). Dashed lines represent final prediction accuracy for the other phylogenetic inference methods. For the low LBA case (left:  $a = 2, b = c = 1$ ), all methods reach 100% accuracy quite fast while for the other two cases: medium LBA (center:  $a = 10, b = c = 1$ ) and high LBA (right:  $a = 40, b = c = 1$ ), all standard phylogenetic methods (NJ, ML, BI) have a 0% accuracy and the two NN models (Zou in dashed pink line and our OptLSTM model in solid yellow line) have a higher accuracy than the naive random prediction (dotted gray line at 33%). We note that our method outperforms Zou’s NN.

to 15, lowering the naive prediction to 6%, marked by the blue dashed line in Fig. 6. Thus, the model has reasonable performance given the number of classes it is trying to classify from.

#### 4 Analysis of Zika virus data

Six viral aminoacid sequences for Zika virus were downloaded using NCBI [34] (query link in GitHub repository <https://github.com/crs14/mn-phylogenetics>). See Table 1 for more details on the sequences. We estimate the best quartet tree for every combination of four taxa (15 combinations) with our OptLSTM NN model and then merge all the predicted quartets into a 6-taxon tree using Quartet MaxCut [35]. For this case, we train our NN model on a heterogeneous dataset that includes all different scenarios of  $a, b, c$  described in the simulations (total sample size 27000). The heterogeneous dataset is constructed by 1000 samples from all different scenarios of  $a, b, c$  dataset, and has 27000 samples in total. Then, we train our NN model on sequentially selected 2000 samples for each epoch and test on newly collected 50 samples at random for each LBA dataset. The training dynamics of our model are shown in Fig. 7 (top and center).

Unlike the default tree built in NCBI [34] that puts *Macaca mulatta* within the *Homo sapiens* clade, our method recovers the expected pattern of divergences with *Macaca mulatta* as sister to *Homo*

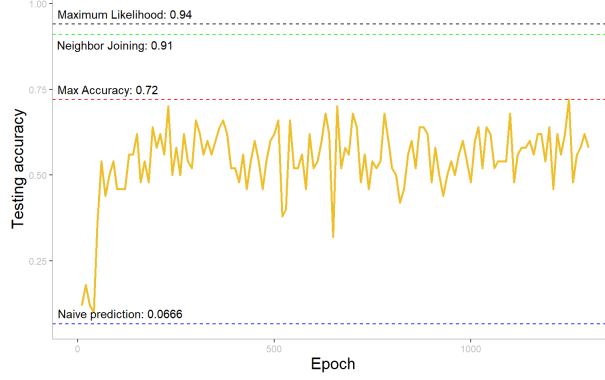


Figure 6: Testing accuracy of all 1300 epochs. The black dashed line indicates the result of the Maximum Likelihood method; the green dashed line indicates the result of the Neighbor-Joining method; the red dashed line indicates the maximum accuracy achieved among all epochs; the blue dashed line indicates the random naive prediction.

Table 1: Zika viral aminoacid sequences downloaded from NCBI [34].

Accession	Length	Host	Country	Year
QIH53581	3423	<i>Homo sapiens</i>	Brazil	2017
BAP47441	3423	<i>Simiiformes</i>	Uganda	1947
ANG09399	3423	<i>Homo sapiens</i>	Honduras	2016
AXF50052	3423	<i>Mus Musculus</i>	Colombia	2016
AWW21402	3423	<i>Simiiformes</i>	Cambodia	2016
AYI50274	3423	<i>Macaca mulatta</i>		2015

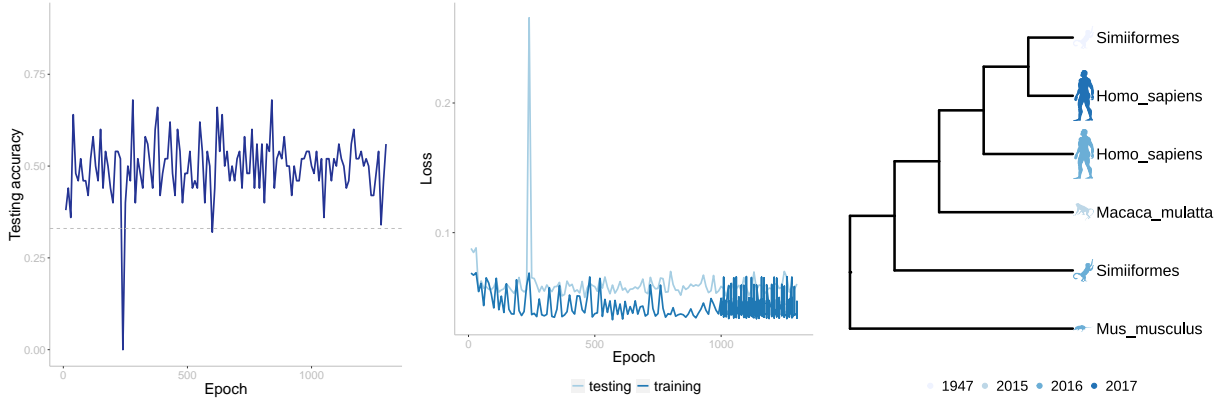


Figure 7: Testing accuracy (top) and training/testing loss (center) of our NN model (OptLSTM) by epoch using the heterogeneous dataset (combining all simulated datasets into one). Dashed line represents expected accuracy naive prediction at random (33% for three quartet options). This trained model was used to estimate all possible quartets in the Zika viral dataset. Bottom: Estimated phylogenetic Zika virus tree using our OptLSTM model in conjunction with Quartet Maxcut [35]. Color of the taxon images represents the sequencing year of the Zika virus.

*sapiens* and *Simiiformes* as an outgroup within the primates clade (Fig. 7). Accession BAP47441 (*Simiiformes*) is the only sequence that does not fit the expected tree structure by appearing in

the middle of the *Homo sapiens* clade. By ignoring this sequence, our estimated tree recovers the *Homo sapiens* clade as expected. We point out that accession BAP47441 is the oldest virus sequenced in this dataset (with sequencing year of 1947) compared to all the other accessions that were sequenced after 2015. It is plausible that the erroneous position of accession BAP47441 is due to incongruences on sequencing technologies between this sequence and the other sequences in the data. While the training of the NN model is not fast (around 3 days), the trained model can be used to predict any number of quartets allowing scientists to estimate trees of whatever size in conjunction with Quartet Maxcut [35] (available at the GitHub repository, see Open-source implementation).

## 5 Discussion

We present here the first neural network model that fully exploits the symmetries of trees to avoid permutation operations as other neural models do in phylogenetics [15]. We showed that our method outperforms standard phylogenetic inference methods like distance-based (NJ), likelihood (ML) and Bayesian (BI) in cases related to LBA, yet it lags behind in the case of five taxa.

While it is difficult to justify the existence of a model that underperforms compared to other phylogenetic inference methods, we argue that the novelty in the mathematical definition of our model is still worthy of recognition. Even when the accuracy of our model to infer 5-taxon trees is below standard phylogenetic methods such as maximum likelihood or neighbor joining, our model is still accurate despite the complexity of the classification task. Furthermore, our model is more efficient in terms of memory and computing time compared to other deep learning implementations. Last, our model is the only existing mathematical representation of a neural network model that intrinsically exploits the tree symmetries, property that can open the door to more complex – yet efficient – models in the future.

For example, the main limitation of existing neural network classifiers in phylogenetics [13, 14, 15] is that inference is possible only for 4-taxon datasets. Unlike other neural network models, however, our model manages to extend the inference task to 5-taxon trees given the built-in invariance to tree permutations. Zou *et al* [15] account for these tree isomorphisms by explicitly adding more samples with all the possible permutations of the sequences ( $4! = 24$  permutations). This data extension imposes demanding memory requirements which become unsustainable for more taxa in the data. Our model, on the contrary, accounts for the tree isomorphisms internally via invariant descriptors which is memory efficient as the number of taxa increases.

Here, we also shed light into the infeasibility of neural network classifiers for larger trees. The limitation of all existing NN classifiers is that it is very hard to go beyond 5-taxon trees, as our model is an optimized complete search of the tree space. For 6-taxon trees, the tree space is 105, while for bigger trees such as 10-taxon trees, the tree space is 2,027,025. It quickly becomes infeasible in terms of computation time and resources for deep Learning models to search the whole tree space. Recently Smith *et al* [17] proposed a General Adversarial Network (GAN) that does a heuristic search approach of tree space without visiting all possible trees. This approach is very similar to standard phylogenetic inference methods and has achieved good results for up to 10 taxon trees. Future developments of deep learning models for phylogenetic inference should follow this direction by avoiding searching the complete tree space. Another direction would be deep learning models that are designed to work with non-Euclidean space, namely the Graph Neural Network (GNN) [36, 37, 38, 39]. Such models would more effectively learn the tree topologies of phylogenetic datasets and could potentially offer better performance compared to existing classifiers, which mostly transform phylogenetic trees into Euclidean space datasets and feed into a conventional Deep Learning model such as CNN and RNN.

In addition to extending the model to more taxa, future work will also involve allowing for nucleotide sequences as input in addition to proteins. Currently, our model is only suited to handle protein sequences so that we could compare our performance to [15]. The other two neural network models applied to phylogenetics [13, 14] use nucleotide sequences as input, so we were unable to compare

them to our model. Thus, one future extension of our model could be the modification of the model to allow for the set of nucleotides to be used as the dictionary for the sequences. Furthermore, Suvorov *et al* [14] allow for gaps in the alignment and proved that a neural network model is better suited to handle highly gapped sequences (which are quite common on bacterial or viral sequences due to difficulty of alignment) compared to standard phylogenetic methods. Therefore, another extension of our model will be the incorporation of gaps in the sequences to test its performance to a variety of gap scenarios.

## Data Availability

All the scripts for the model implementation, simulations and real data analysis can be found in the GitHub repository: <https://github.com/crs14/nn-phylogenetics>.

## Acknowledgements

This work was partially supported by the Department of Energy [DE-SC0021016 to C. S.-L.], National Science Foundation [DEB-2144367 to CSL] and the National Science Foundation [DMS-2012292 to L. Z.-N.].

## References

- [1] B. Groombridge. Global biodiversity: status of the Earth's living resources. *World Conservation Monitoring Centre*, 1992.
- [2] M. D. Hendy and D. Penny. A framework for the quantitative study of evolutionary trees. *Systematic zoology*, 38(4):297–309, 1989.
- [3] J. Felsenstein. Cases in which parsimony or compatibility methods will be positively misleading. *Systematic zoology*, 27(4):401–410, 1978.
- [4] J. Bergsten. A review of long-branch attraction. *Cladistics*, 21(2):163–193, 2005.
- [5] F. E. Anderson and D. L. Swofford. Should we be worried about long-branch attraction in real data sets? Investigations using metazoan 18S rDNA. *Molecular phylogenetics and evolution*, 33(2):440–451, 2004.
- [6] J. Gauthier, A. G. Kluge, and T. Rowe. Amniote phylogeny and the importance of fossils. *Cladistics*, 4(2):105–209, 1988.
- [7] J. J. Wiens. Can incomplete taxa rescue phylogenetic analyses from long-branch attraction? *Systematic Biology*, 54(5):731–742, 2005.
- [8] J. Felsenstein and J. Felsenstein. *Inferring phylogenies*, volume 2. Sinauer associates Sunderland, MA, 2004.
- [9] J. P. Huelsenbeck and D. M. Hillis. Success of phylogenetic methods in the four-taxon case. *Systematic Biology*, 42(3):247–264, 1993.
- [10] H. Philippe, Y. Zhou, H. Brinkmann, N. Rodrigue, and F. Delsuc. Heterotachy and long-branch attraction in phylogenetics. *BMC evolutionary biology*, 5(1):1–8, 2005.
- [11] N. Lartillot and H. Philippe. A Bayesian mixture model for across-site heterogeneities in the amino-acid replacement process. *Molecular biology and evolution*, 21(6):1095–1109, 2004.
- [12] N. Lartillot, H. Brinkmann, and H. Philippe. Suppression of long-branch attraction artefacts in the animal phylogeny using a site-heterogeneous model. *BMC evolutionary biology*, 7(1):1–14, 2007.
- [13] A. F. Leuchtenberger, S. M. Crotty, T. Drucks, H. A. Schmidt, S. Burgstaller-Muehlbacher, and A. von Haeseler. Distinguishing Felsenstein Zone from Farris Zone Using Neural Networks. *Molecular Biology and Evolution*, 37(12):3632–3641, December 2020.

- [14] A. Suvorov, J. Hochuli, and D. R. Schrider. Accurate Inference of Tree Topologies from Multiple Sequence Alignments Using Deep Learning. *Syst. Biol.*, 69(2):221–233, March 2020.
- [15] Z. Zou, H. Zhang, Y. Guan, and J. Zhang. Deep Residual Neural Networks Resolve Quartet Molecular Phylogenies. *Mol. Biol. Evol.*, 37(5):1495–1507, May 2020.
- [16] K. Strimmer and A. Von Haeseler. Quartet puzzling: a quartet maximum-likelihood method for reconstructing tree topologies. *Molecular biology and evolution*, 13(7):964–969, 1996.
- [17] M. L. Smith and M. W. Hahn. Phylogenetic inference using Generative Adversarial Networks. *bioRxiv*, 2023.
- [18] M. Zaheer, S. Kottur, S. Ravanbakhsh, B. Poczos, R. R. Salakhutdinov, and A. J. Smola. Deep sets. pages 3391–3401, 2017.
- [19] K. He, X. Zhang, S. Ren, and J. Sun. Deep residual learning for image recognition. In *Proceedings of the IEEE conference on computer vision and pattern recognition*, pages 770–778, 2016.
- [20] S. Hochreiter and J. Schmidhuber. Long Short-Term Memory. *Neural Computation*, 9(8):1735–1780, 11 1997.
- [21] D. Kingma and J. Ba. Adam: A method for stochastic optimization. In *The 3rd International Conference for Learning Representations (ICLR)*, 2015. arXiv:1412.6980v8.
- [22] A. Paszke, S. Gross, F. Massa, A. Lerer, J. Bradbury, G. Chanan, T. Killeen, Z. Lin, N. Gimelshein, L. Antiga, A. Desmaison, A. Kopf, E. Yang, Z. DeVito, M. Raison, A. Tejani, S. Chilamkurthy, B. Steiner, L. Fang, J. Bai, and S. Chintala. PyTorch: An Imperative Style, High-Performance Deep Learning Library. In H. Wallach, H. Larochelle, A. Beygelzimer, F. d’Alché-Buc, E. Fox, and R. Garnett, editors, *Advances in Neural Information Processing Systems 32*, pages 8024–8035. Curran Associates, Inc., 2019.
- [23] J. Felsenstein. Cases in which Parsimony or Compatibility Methods will be Positively Misleading. *Syst. Biol.*, 27(4):401–410, December 1978.
- [24] Z. Yang, R. Nielsen, and M. Hasegawa. Models of amino acid substitution and applications to mitochondrial protein evolution. *Mol. Biol. Evol.*, 15(12):1600–1611, December 1998.
- [25] Z. Yang. PAML 4: phylogenetic analysis by maximum likelihood. *Mol. Biol. Evol.*, 24(8):1586–1591, August 2007.
- [26] M. O. Dayhoff and R. M. Schwartz. Chapter 22: A model of evolutionary change in proteins. *Atlas of Protein Sequence and Structure*, 1978.
- [27] E. Paradis and K. Schliep. ape 5.0: an environment for modern phylogenetics and evolutionary analyses in R. *Bioinformatics*, 35:526–528, 2019.
- [28] N. Saitou and M. Nei. The neighbor-joining method: a new method for reconstructing phylogenetic trees. *Molecular biology and evolution*, 4(4):406–425, 1987.
- [29] J. A. Studier and K. J. Keppler. A note on the neighbor-joining algorithm of Saitou and Nei. *Molecular biology and evolution*, 5(6):729–731, 1988.
- [30] A. Stamatakis. RAxML version 8: a tool for phylogenetic analysis and post-analysis of large phylogenies. *Bioinformatics*, 30(9):1312–1313, 2014.
- [31] J. P. Huelsenbeck and F. Ronquist. MRBAYES: Bayesian inference of phylogenetic trees. *Bioinformatics*, 17(8):754–755, 2001.
- [32] F. Ronquist and J. P. Huelsenbeck. MrBayes 3: Bayesian phylogenetic inference under mixed models. *Bioinformatics*, 19(12):1572–1574, 2003.
- [33] N. S. Keskar, D. Mudigere, J. Nocedal, M. Smelyanskiy, and P. T. P. Tang. On Large-Batch Training for Deep Learning: Generalization Gap and Sharp Minima. *CoRR*, abs/1609.04836, 2016.
- [34] National Center for Biotechnology Information. <https://www.ncbi.nlm.nih.gov/>. Accessed: 2021-11-20.

- [35] S. Snir and S. Rao. Quartet MaxCut: a fast algorithm for amalgamating quartet trees. *Molecular phylogenetics and evolution*, 62(1):1–8, 2012.
- [36] C. Zhang. Learnable Topological Features for Phylogenetic Inference via Graph Neural Networks, 2023.
- [37] W. Jin, R. Barzilay, and T. Jaakkola. Junction Tree Variational Autoencoder for Molecular Graph Generation. In J. Dy and A. Krause, editors, *Proceedings of the 35th International Conference on Machine Learning*, volume 80 of *Proceedings of Machine Learning Research*, pages 2323–2332. PMLR, 10–15 Jul 2018.
- [38] D. Jiang, Z. Wu, C.-Y. Hsieh, G. Chen, B. Liao, Z. Wang, C. Shen, D. Cao, J. Wu, and T. Hou. Could graph neural networks learn better molecular representation for drug discovery? A comparison study of descriptor-based and graph-based models. *Journal of Cheminformatics*, 13(1):12, Feb 2021.
- [39] Y. Kwon, J. Yoo, Y.-S. Choi, W.-J. Son, D. Lee, and S. Kang. Efficient learning of non-autoregressive graph variational autoencoders for molecular graph generation. *Journal of Cheminformatics*, 11(1):70, Nov 2019.